KKU Res. J. 2012; 17(3):338-347
http : //resjournal.kku.ac.th

A Novel IIR Equalizer Design for Perpendicular Recording Systems with Media Jitter Noise

Chanon Warisarn[1]*, *Piya Kovintavewat*[2], *Pornchai Supnithi*[3]

[1] *College of Data Storage Innovation, King Mongkut's Institute of Technology Ladkrabang*
[2] *Data Storage Technology Research Center, Nakhon Pathom Rajabhat University*
[3] *Telecommunications Engineering Department, King Mongkut's Institute of Technology Ladkrabang*
* *Correspondent author: kwchanon@kmitl.ac.th*

Received February 7, 2012
Accepted April 15, 2012

Abstract

In this paper, a method of designing an infinite impulse response (IIR) equalizer for turbo equalization in the perpendicular magnetic recording channels will be designed and described. Based on a minimum mean-squared error (MMSE) approach, the coefficients of the IIR equalizer are explicitly derived. Then, we compare its performance with a finite-impulse response (FIR) equalizer in the presence and absence of the media jitter noise. Results indicate that for a small number of equalizer taps, the proposed IIR equalizer outperforms the FIR equalizer at moderate to high jitter noise levels. Also if compared with an 11-tap FIR equalizer, the proposed IIR counterpart can achieve a similar BER performance, but it requires a fewer number of equalizer taps.

1. Introduction

The PRML technique (1) is widely used for data detection process in the perpendicular magnetic recording channels. In practice, in this technique, an FIR equalizer is employed to shape the readback signal to a predetermined target before performing maximum-likelihood (ML) equalization by the Viterbi detector (2).

The FIR equalizer with a large number of taps is required to function properly at high recording densities. Nevertheless, the total number of equalizer taps is practically limited by the maximum allowable loop delay in the timing recovery loop because a small loop delay provides a more robust phase locking (3), which in turn improves the overall system performance. Furthermore, the benefits of the equalizer with fewer taps are three folds. (i) A smaller area on the silicon chip. (ii) A shorter optimization time of read-channel chip during the production. (iii) A small delay in the timing loop.

An IIR equalizer has previously been studied in the literature (4) and references therein. For instance, the IIR modeling was considered in the decision feedback equalizer design (5) to reduce the number of filter taps. Also, in (6), the performance of employing the continuous-time adaptive IIR equalizers for EPR4 channels was investigated.

An algorithm for the approximation of FIR filter by the IIR filter and the direct method for converting the FIR filter with low non-zero taps into the IIR filter using the predetermined table are proposed in (7 – 8), respectively. However, in this paper, we directly design the digital IIR equalizer based on the MMSE approach, and then compare its performance with the conventional FIR equalizer in a full turbo equalization setting.

The rest of this paper is organized as follows. After explaining our system model in Section 2, we briefly explain the design of the conventional FIR equalizer, and also describe the design of the IIR equalizers for partial response channels in Section 3. Simulation results are provided in Section 4. Finally, summary is given in Section 5.

2. System Model

Figure 1 illustrates the channel model of a perpendicular magnetic recording system with jitter noise. A message input sequence $u_k \epsilon \{0,1\}$ is encoded by a low-density parity-check (LDPC) code and is mapped to a binary input sequence $x_k \epsilon \{\pm 1\}$ with a bit period T, Then, the sequence x_k is filtered by an ideal differentiator 1-D to form a transition sequence $c_k = \{x_k - x_{k-1}\}$ where $c_k = \pm 2$ corresponds to a positive or negative transition and $c_k = 0$ corresponds to the absence of a transition. The sequence c_k is then passed through the perpendicular recording channel, represented by the transition response $g(t)$ of the form (3)

$$g(t) = \mathrm{erf}\left(\frac{t\sqrt{\ln 16}}{PW_{50}}\right), \qquad [1]$$

where $\mathrm{erf}(x) = \left(2/\sqrt{\pi}\right)\int_0^x e^{-t^2} dt$ is an error function, and PW_{50} is the width of the derivative of $g(t)$ at half of its maximum. We define a normalized recording density (ND) as ND=PW_{50} / T, which determines how many data bits can be packed within the resolution unit PW_{50}.

The readback signal $p(t)$ in Figure 1 can be expressed as

$$p(t) = \sum_k c_k g(t - kT + \Delta t_k) + n(t), \qquad [2]$$

where $n(t)$ is an additive white Gaussian noise (AWGN) with the two-sided power spectral density of $N_0/2$ (W/Hz). The jitter noise Δt_k is modeled as a truncated Gaussian probability distribution function with

$\mathcal{N}\left(0,\ |c_k|\sigma_j^2\right)$, where σ_j specified as a percentage of T determines the severity of the jitter noise.

The sampled output s_k is equalized by a digital equalizer of the form

$$F_{FIR}(D)=\sum_{k=-K}^{K} f_k D^k \ , \qquad [3]$$

where f_k is the k-th equalizer coefficients, and $2K+1$ is the total number of equalizer taps, such that the output sequence y_k resembles the desired target output sequence d_k. Finally, the sequence y_k is fed to a turbo equalizer, which iteratively exchanges the soft information between the soft output SOVA equalizer (9) and the LDPC decoder, respectively.

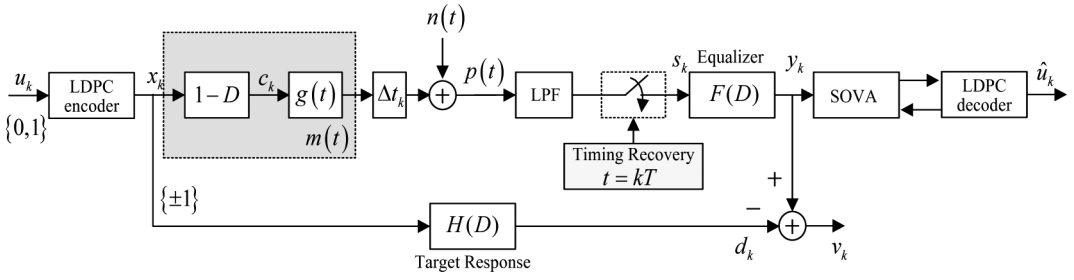

Figure 1. System model for turbo equalization and target design.

3. Target and Equalizer Design

3.1 MMSE FIR Equalizer

A typical MMSE FIR filter design is based on Figure 1. Consider a partial-response target of the form

$$H(D)=\sum_{k=0}^{L-1} h_k D^k \ , \qquad [4]$$

where L is the target length, and h_k is the k-th target coefficients. From Figure 1, the equalizer output and the target output are expressed as

$$y_k = s_k * f_k, \qquad [5]$$

and

$$d_k = x_k * h_k, \qquad [6]$$

respectively, where * denotes the convolution operator. Equation [5] and [6] can also be written in the matrix form as

$$y_k = \mathbf{f}^{\mathrm{T}}\mathbf{s}, \qquad [7]$$

and

$$d_k = \mathbf{h}^{\mathrm{T}}\mathbf{x}, \qquad [8]$$

where $\mathbf{f}=\left[f_{-K}, f_{-K+1},\ldots, f_{K-1}, f_K\right]^{\mathrm{T}}$, $\mathbf{s}=\left[s_{k+K}, s_{k+K-1},\ldots, s_{k-K}\right]^{\mathrm{T}}$, $\mathbf{h}=\left[h_0, h_1,\ldots, h_{L-1}\right]^{\mathrm{T}}$, $\mathbf{x}=\left[x_k, x_{k-1},\ldots, x_{k-L+1}\right]^{\mathrm{T}}$, and $\left[\bullet\right]^{\mathrm{T}}$ is the transpose operation. Note that in this paper the bold characters denoted as the matrix, and italic characters denoted as the parameter. The target and its corresponding FIR equalizer can then be simultaneously obtained based on a minimum mean-square error (MMSE) approach. The mean-square error (MSE) between the equalizer output y_k and the target output d_k is given by (10)

$$E\left[v_k^2\right]=E\left[\left(y_k-d_k\right)^2\right] = \mathbf{f}^{\mathrm{T}}\mathbf{R}\mathbf{f}+\mathbf{h}^{\mathrm{T}}\mathbf{A}\mathbf{h}-2\mathbf{f}^{\mathrm{T}}\mathbf{P}\mathbf{h}, \qquad [9]$$

where $E[\bullet]$ is the expectation operator, $\mathbf{R} = E[\mathbf{s}\mathbf{s}^{\mathrm{T}}]$ is an *N*-by-*N* auto-correlation matrix of the sampled channel output s_k, $\mathbf{A} = E[\mathbf{x}\mathbf{x}^{\mathrm{T}}]$ is an *L*-by-*L* auto-correlation matrix of the input sequence x_k, and x_k, and $\mathbf{P} = E[\mathbf{s}\mathbf{x}^{\mathrm{T}}]$ is an *N*-by-*L* cross-correlation matrix between s_k and x_k.

Given a specified constraint, the MSE in [9] can be minimized by differentiating [9] with respect to **h** and **f**, and setting the results to zero. For a fixed partial-response target **h**, the equalizer coefficients can be computed from

$$\mathbf{f} = \mathbf{R}^{-1}\mathbf{P}\mathbf{h}. \qquad [10]$$

Alternative method to obtain the FIR filter coefficients is based on the neural network (11-12). The extended Kalman filter (EKF) algorithms based on the real-time recurrent learning (RTRL) for the decision feedback recurrent neural equalizer (DFRNE) was proposed in (11) to solve drawback of slow convergence rate. Then, a new design method of the simplified neural network equalizer (NNE) with the noise whitening function was proposed in (12) for a generalized partial response (GPR) channel is proposed.

3.2 MMSE IIR Equalizer

The method for designing the proposed IIR equalizer can be described by a block diagram as shown in Figure 2. An IIR equalizer *F(D)* is expressed as (4)

$$F(D) = \frac{B(D)}{A(D)} = \frac{\sum_{k=-N}^{N} b_k D^k}{\sum_{k=0}^{M} a_k D^k}, \qquad [11]$$

where a_k and b_k are the *k*-th coefficients of the denominator and the numerator of *F(D)* respectively, and both *N* and *M* are integers. In our study, we consider the case where *M+1<2N+1*. From Figure 2, we see that

$$y_k = s_k * f_k, \qquad [12]$$

which can be rewritten as

$$s_k * b_k = y_k * a_k. \qquad [13]$$

By substituting $y_k = d_k + v_k$ into (13), we obtain

$$s_k * b_k = (d_k + v_k) * a_k,$$
$$v_k * a_k = s_k - d_k * a_k. \qquad [14]$$

Assuming that $a_0 = 1$, [14] can be written as

$$v_k + \sum_{i=1}^{M} v_{k-i} a_i = s_k * b_k - d_k * a_k, \qquad [15]$$

and

$$v_k = s_k * b_k - \left(d_k + \sum_{i=1}^{M} d_{k-i} a_i \right) - \sum_{i=1}^{M} v_{k-i} a_i \qquad [16]$$
$$= s_k * b_k - \tilde{d}_k * \tilde{a}_k - \tilde{v}_k * \tilde{a}_k - d_k.$$

For convenience, [16] can be written in the matrix form as

$$v_k = \mathbf{s}^{\mathrm{T}}\mathbf{b} - \tilde{\mathbf{d}}^{\mathrm{T}}\tilde{\mathbf{a}} - \tilde{\mathbf{v}}^{\mathrm{T}}\tilde{\mathbf{a}} - d_k, \qquad [17]$$

where $\mathbf{s} = [s_{k+N}, ..., s_k, ..., s_{k-N}]^{\mathrm{T}}$, $\mathbf{b} = [b_{-N}, ..., b_0, ..., b_N]^{\mathrm{T}}$, $\tilde{\mathbf{d}} = [d_{k-1}, d_{k-2}, ..., d_{k-M}]^{\mathrm{T}}$, $\tilde{\mathbf{a}} = [a_1, ..., a_M]^{\mathrm{T}}$, and $\tilde{\mathbf{v}} = [v_{k-1}, v_{k-2}, ..., v_{k-M}]^{\mathrm{T}}$ are *(2N+1)*, *(2N+1)*, *M*, *M*, and *M*-element column vector, respectively. Then, the MSE of [17] is given by

$$\begin{aligned} E[v_k^2] &= E\left[\left(\mathbf{b}^{\mathrm{T}}\mathbf{s} - \tilde{\mathbf{a}}^{\mathrm{T}}\tilde{\mathbf{d}} - \tilde{\mathbf{a}}^{\mathrm{T}}\tilde{\mathbf{v}} - d_k \right) \left(\mathbf{s}^{\mathrm{T}}\mathbf{b} - \tilde{\mathbf{d}}^{\mathrm{T}}\tilde{\mathbf{a}} - \tilde{\mathbf{v}}^{\mathrm{T}}\tilde{\mathbf{a}} - d_k \right) \right] \\ &= E\left[\mathbf{b}^{\mathrm{T}}\mathbf{s}\mathbf{s}^{\mathrm{T}}\mathbf{b} - \mathbf{b}^{\mathrm{T}}\mathbf{s}\tilde{\mathbf{d}}^{\mathrm{T}}\tilde{\mathbf{a}} - \mathbf{b}^{\mathrm{T}}\mathbf{s}\tilde{\mathbf{v}}^{\mathrm{T}}\tilde{\mathbf{a}} - \mathbf{b}^{\mathrm{T}}\mathbf{s}d_k \right. \\ &\quad - \tilde{\mathbf{a}}^{\mathrm{T}}\tilde{\mathbf{d}}\mathbf{s}^{\mathrm{T}}\mathbf{b} - \tilde{\mathbf{a}}^{\mathrm{T}}\tilde{\mathbf{d}}\tilde{\mathbf{d}}^{\mathrm{T}}\tilde{\mathbf{a}} - \tilde{\mathbf{a}}^{\mathrm{T}}\tilde{\mathbf{d}}\tilde{\mathbf{v}}^{\mathrm{T}}\tilde{\mathbf{a}} - \tilde{\mathbf{a}}^{\mathrm{T}}\tilde{\mathbf{d}}d_k \\ &\quad - \tilde{\mathbf{a}}^{\mathrm{T}}\tilde{\mathbf{v}}\mathbf{s}^{\mathrm{T}}\mathbf{b} - \tilde{\mathbf{a}}^{\mathrm{T}}\tilde{\mathbf{v}}\tilde{\mathbf{d}}^{\mathrm{T}}\tilde{\mathbf{a}} - \tilde{\mathbf{a}}^{\mathrm{T}}\tilde{\mathbf{v}}\tilde{\mathbf{v}}^{\mathrm{T}}\tilde{\mathbf{a}} - \tilde{\mathbf{a}}^{\mathrm{T}}\tilde{\mathbf{v}}d_k \\ &\quad \left. - d_k\mathbf{s}^{\mathrm{T}}\mathbf{b} - d_k\tilde{\mathbf{d}}^{\mathrm{T}}\tilde{\mathbf{a}} - d_k\tilde{\mathbf{v}}^{\mathrm{T}}\tilde{\mathbf{a}} - d_k d_k \right] \end{aligned} \qquad [18]$$

given $\mathbf{c} = E[\mathbf{s}d_k]$, $\mathbf{d} = E[\tilde{\mathbf{d}}d_k]$, $\mathbf{e} = E[\tilde{\mathbf{v}}d_k]$ are *(2N+1)*, *M*, *M*, and *M*-element column vectors, respectively. We can rearrange (18) as

$$\begin{aligned} E[v_k^2] &= \mathbf{b}^{\mathrm{T}}\mathbf{S}\mathbf{b} - \mathbf{b}^{\mathrm{T}}\mathbf{X}\tilde{\mathbf{a}} - \mathbf{b}^{\mathrm{T}}\mathbf{P}\tilde{\mathbf{a}} - \mathbf{b}^{\mathrm{T}}\mathbf{c} - \tilde{\mathbf{a}}^{\mathrm{T}}\mathbf{X}^{\mathrm{T}}\mathbf{b} + \tilde{\mathbf{a}}^{\mathrm{T}}\mathbf{D}\tilde{\mathbf{a}} \\ &\quad + \tilde{\mathbf{a}}^{\mathrm{T}}\mathbf{W}\tilde{\mathbf{a}} + \tilde{\mathbf{a}}^{\mathrm{T}}\mathbf{d} - \tilde{\mathbf{a}}^{\mathrm{T}}\mathbf{P}^{\mathrm{T}}\mathbf{b} + \tilde{\mathbf{a}}^{\mathrm{T}}\mathbf{W}^{\mathrm{T}}\tilde{\mathbf{a}} + \tilde{\mathbf{a}}^{\mathrm{T}}\mathbf{V}^{\mathrm{T}}\tilde{\mathbf{a}} \\ &\quad + \tilde{\mathbf{a}}^{\mathrm{T}}\mathbf{e} - \mathbf{c}^{\mathrm{T}}\mathbf{b} + \mathbf{d}^{\mathrm{T}}\tilde{\mathbf{a}} + \mathbf{e}^{\mathrm{T}}\tilde{\mathbf{a}} + d_k^2 \end{aligned} \qquad [19]$$

where $\mathbf{S} = E[\mathbf{s}\mathbf{s}^{\mathrm{T}}]$, $\mathbf{X} = E[\mathbf{s}\tilde{\mathbf{d}}^{\mathrm{T}}]$, $\mathbf{P} = E[\mathbf{s}\tilde{\mathbf{v}}^{\mathrm{T}}]$, $\mathbf{D} = E[\tilde{\mathbf{d}}\tilde{\mathbf{d}}^{\mathrm{T}}]$, $\mathbf{W} = E[\tilde{\mathbf{d}}\tilde{\mathbf{v}}^{\mathrm{T}}]$, and $\mathbf{V} = E[\tilde{\mathbf{v}}\tilde{\mathbf{v}}^{\mathrm{T}}]$

are (*2N+1*)-by-(*2N+1*), (*2N+1*)-by-*M*, (*2N+1*)-by-*M*, *M*-by-*M*, *M*-by-*M*, and *M*-by-*M*, matrices, respectively.

To find the coefficients of an IIR equalizer, we differentiate [19] with respect to $\tilde{\mathbf{a}}$ and $\mathbf{b}$, respectively, and set the results to zero, to obtain

$$\frac{\partial E\left[v_k^2\right]}{\partial \tilde{\mathbf{a}}} = 2\mathbf{S}\mathbf{b} - 2\mathbf{X}\tilde{\mathbf{a}} - 2\mathbf{P}\tilde{\mathbf{a}} - 2\mathbf{c} = 0, \qquad [20]$$

and

$$\frac{\partial E\left[v_k^2\right]}{\partial \mathbf{b}} = 2\mathbf{X}^{\mathrm{T}}\mathbf{b} - 2\mathbf{P}^{\mathrm{T}}\mathbf{b} + 2\mathbf{D}\tilde{\mathbf{a}} + 2\mathbf{W}\tilde{\mathbf{a}} + 2\mathbf{d} + 2\mathbf{W}^{\mathrm{T}}\tilde{\mathbf{a}} + 2\mathbf{V}\tilde{\mathbf{a}} + 2\mathbf{e} = 0. \qquad [21]$$

An equivalent matrix suited for calculation is obtained by rearranging [20] and [21] as

$$\underbrace{\begin{bmatrix} \mathbf{S} & -[\mathbf{X}+\mathbf{P}] \\ -\mathbf{X}^{\mathrm{T}} & \mathbf{D}+\mathbf{W}+\mathbf{W}^{\mathrm{T}}+\mathbf{V} \end{bmatrix}}_{\mathbf{Q}} \underbrace{\begin{bmatrix} \mathbf{b} \\ \tilde{\mathbf{a}} \end{bmatrix}}_{\mathbf{z}} = \underbrace{\begin{bmatrix} \mathbf{c} \\ -[\mathbf{d}+\mathbf{e}] \end{bmatrix}}_{\mathbf{u}}. \qquad [22]$$

Because the matrix $\mathbf{Q}$ in (22) is a square matrix, the coefficients of *F(D)* in a vector $\mathbf{z}$ can be easily computed from

$$\mathbf{z} = \mathbf{Q}^{-1}\mathbf{u}. \qquad [23]$$

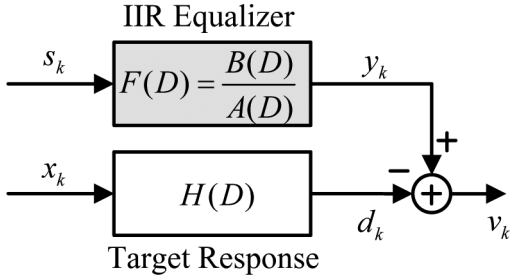

Figure 2. Block diagram for designing an IIR equalizer.

4. Simulation Results and Discussions

We consider the EEPR2 target (13) $H(D) = 1+4D+6D^2+4D^3+D^4$ for perpendicular magnetic recording systems. The (2*K*+1)- tap FIR equalizer is designed based on the MMSE approach, which also yields an error sequence v_k that will be used to design the IIR equalizer. The signal-to-noise ratio (SNR) is defined as

$$\mathrm{SNR}=10\log_{10}\left(\frac{E_i}{N_0}\right)\ (\mathrm{dB}), \qquad [24]$$

where E_i is the energy of the channel impulse response. All equalizers are designed at the SNR required to achieve bit-error rate (BER) = 10^{-5}. Each BER point is computed using as many 4096-bits data sectors as needed to collect 500 error bits, whereas the equalizer taps are designed using only one data sector.

4.1 Uncoded System

First, we consider an uncoded system, where the LDPC encoder and decoder are not used. Thus, we investigate the performance of different equalizers, namely, the FIR equalizers with 3, 5, and 11 taps and the IIR equalizers with 2 and 4 zeros (one pole each) at the output of the SOVA detector.

Figure 3 plots the SNR required to achieve BER = 10^{-4} as a function of NDs in the absence of the jitter noise ($\sigma_j^2 = 0\%$), where the term "*vZmP* IIR" refers to the IIR equalizer with *v=2N* zeros (equivalent to *v*+1 taps) and *m=M* poles. It should be noted that a (*2K+1*) tap FIR filter causes the same amount of delays as a 2*KZmP* IIR filter with 2*K* zeros. As depicted in Figure 3, when the number of equalizer taps is small (e.g., 3 taps) and ND is high, the IIR equalizers with the same delays perform better than the FIR equalizer. It should be noted that the 4*Z*1*P* IIR

filter performs better than the 2*Z*1*P* IIR filter because the equalizer that has more tap numbers can efficiently shape the corresponding signal to the target output better than the equalizer that has less tap numbers.

In Figure 4, we pick ND = 3 and this time compare the performance of different equalizers as a function of the jitter noise amounts from 0% to 6%. It is evident that the 4*Z*2*P* IIR equalizer requires lower SNR to achieve BER = 10^{-4} than both the 5-tap and the 7-tap FIR equalizers. In addition, the 4*Z*2*P* IIR filter performs close to the 11-tap FIR equalizer at all jitter noise levels. From the viewpoint of delays, it can be concluded that the 4*Z*2*P* IIR equalizer is more advantageous than the 11-tap FIR equalizer because it introduces only two delays in the system rather than five delays introduced by the 11-tap FIR equalizer.

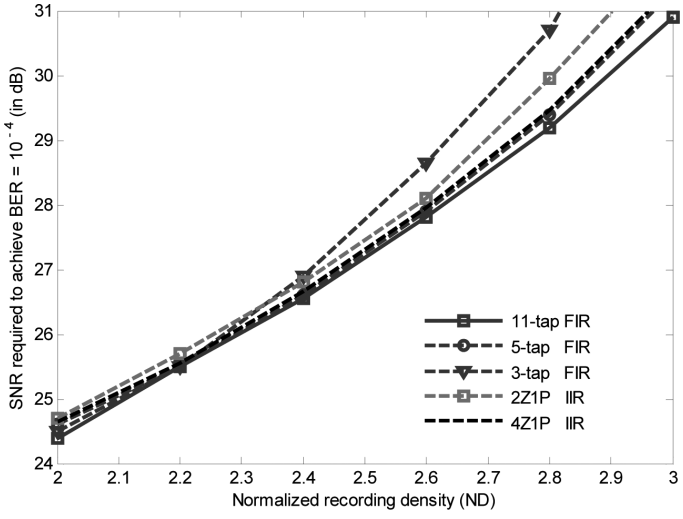

Figure 3. Performance comparisons between the FIR and the IIR equalizers at different NDs.

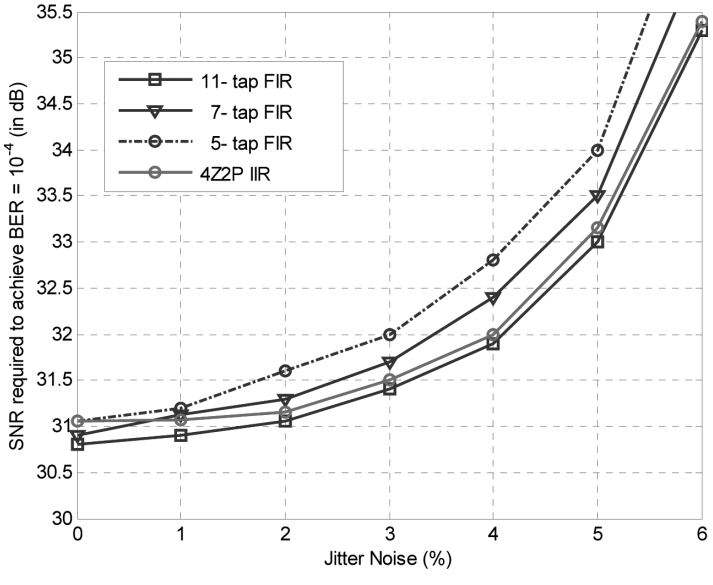

Figure 4. Performance comparisons at different jitter noise levels.

4.2 Coded System

We also investigate the performance of the IIR equalizers in turbo equalization setting for 4 iterations with and without jitter noise as shown in Figure 5. The LDPC code is from a modified array code (MAC) with parameter (p, j, k)=(107, 4, 38) (14). We consider a rate $(1 - j / k)$=0.8947 coded system in which a block of 3,638 message bits $\{u_k\}$ is encoded by an LDPC encoder, resulting in a coded block length of 4,066 bits, and is mapped to an input data sequence $\{x_k\}$ as shown in Figure 1. Similarly, the detected bits are also decoded by the LDPC decoder to obtain an estimated message sequence $\{\hat{u}_k\}$.

To account for the code rate, the user density (D_u) used instead of ND in this simulation, is defined as

$$D_u = \text{ND x R}, \qquad [25]$$

where R = 0.8947 is a code rate for this simulation setup. We also pick ND = 3.0 such that D_u=2.6841. In Figure 5, it is apparent that the 4Z2P IIR filter achieves a similar BER level to the 11-tap FIR filter. In addition, at BER = 10^{-5}, the proposed IIR filter yields the performance gain of 0.2 dB (without jitter noise) and 0.4 dB (with jitter noise 6%) over the 7-tap FIR filter.

The reason that the IIR equalizer provides a better performance than the FIR equalizer because it can shape the readback signal to the PR target better than the FIR equalizer does, especially when the number of equalizer taps is small. This can be explained by plotting the frequency responses of different equalizers in Figure 6 for the perpendicular magnetic recording channel at ND = 3.0. If we assume that the 11-tap FIR equalizer is the best, the 4Z2P IIR equalizer whose frequency response closely matches the frequency response of the 11-tap FIR equalizer than that of the 7-tap FIR equalizer.

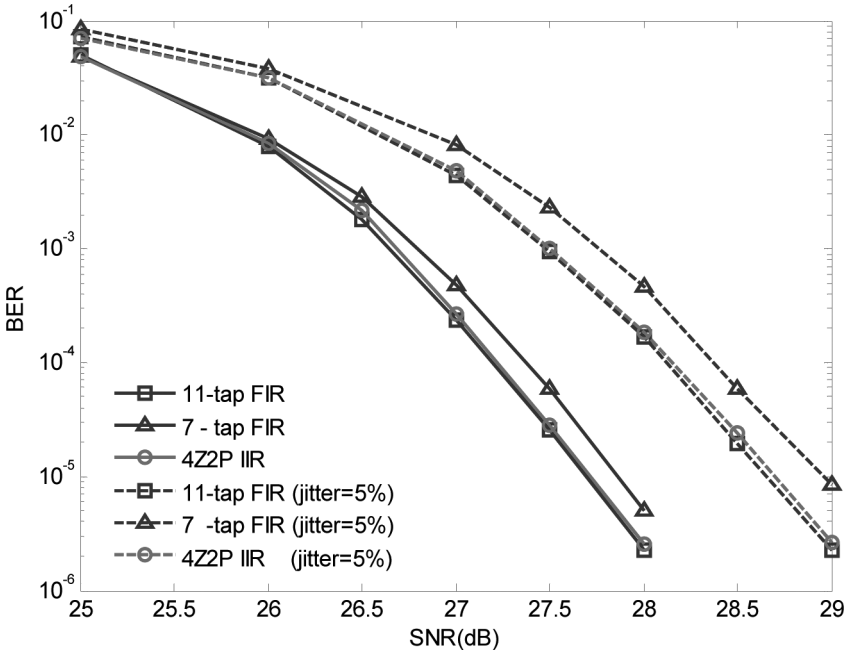

Figure 5. Performance comparisons in the turbo equalization setting with 4 iterations.

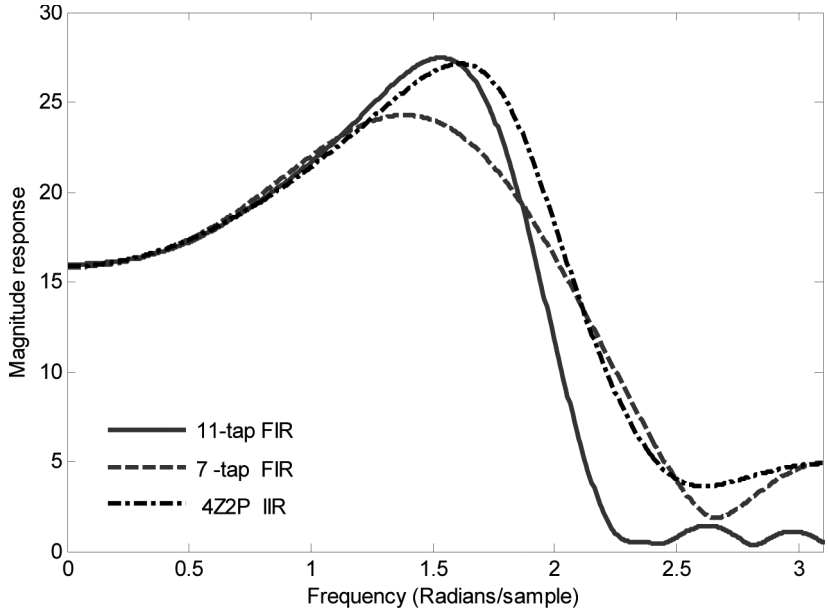

Figure 6. Frequency responses of the readback signals at ND = 3.

4.3 Stable Investigation

Generally, the IIR filter comes with possible concern about stability; however, based on our extensive simulations, we have been able to conclude that the proposed IIR equalizer is highly stable for PR channels. This can be explained by plotting the poles-zeros diagram of the proposed $4Z2P$ IIR equalizer in Figure 7 for the perpendicular magnetic recording channel at ND = 3.0. We can see that theses poles lies inside the unit circle IIR equalizer.

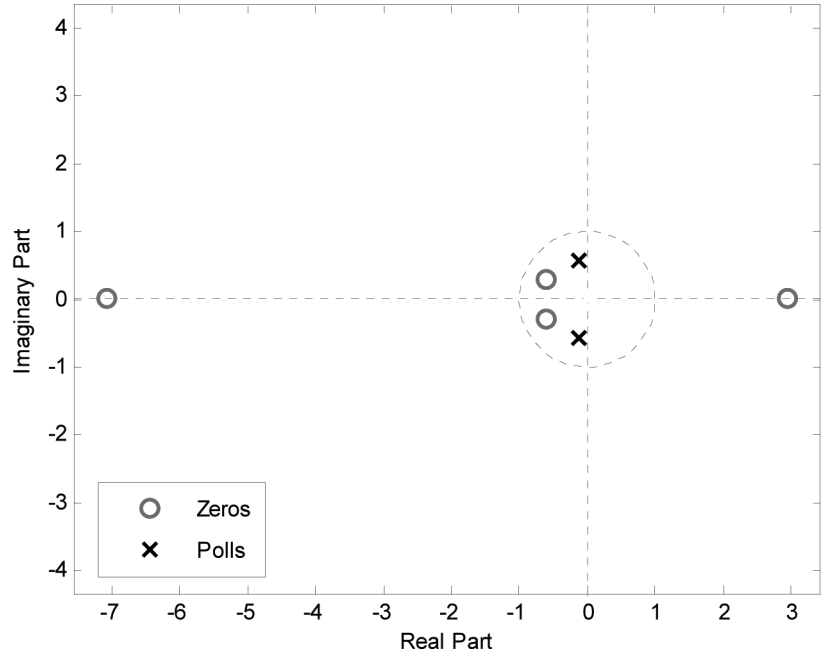

Figure 7. Poles-zeros diagram of the proposed $4Z2P$ IIR equalizer.

5. Summary

In this paper, we propose an IIR equalizer for perpendicular magnetic recording channels based on the MMSE approach. Based on our extensive simulations, we found that the proposed IIR equalizer is highly stable for PR channels. Simulation results show that for small number of equalizer taps, the proposed IIR equalizers with suitable poles and zeroes can outperform the FIR equalizers and also perform close to the 11-tap FIR filter for all jitter noise levels. This is because the IIR equalizer can shape the readback signal to the PR target better than the FIR equalizer. Furthermore, in the turbo equalization setting, we found that the $4Z2P$ IIR filter performs close to the 11-tap FIR filter, and both yields the performance gain of 0.4 dB over the 7-tap FIR filter to achieve the same BER = 10^{-5}.

6. Acknowledgement

This work was supported by College of Data Storage Innovation, King Mongkut's Institute of Technology Ladkrabang, Thailand.

7. References

(1) Cideciyan R. D., Dolivo F., Hermann R., Hirt W., and Schott W. "A PRML System for Digital Magnetic Recording." **IEEE J. Selected Areas Commun.,** vol. 10, Jan. 1992. pp. 38–56.

(2) Forney G. D. "Maximum-likelihood Sequence Estimation of Digital Sequences in The Presence Of Intersymbol Interference." **IEEE Trans. Inform. Theory,** vol. IT-18, May 1972. pp. 363–378.

(3) Bergman J. W. M. **Digital baseband transmission and recording.** Boston, Massachusetts : Kluwer academic publishers. 1996.

(4) Kovintavewat P., Warisarn C., and Supnithi P. "An MMSE Infinite Impulse Response Equalizer for Perpendicular Recording Channels with Jitter Noise." in **Proc. of ITC-CSCC 2008**, **Shimonoseki, Yamagushi, Japan**, Jul. 2008.

(5) Crespo P. M., Honig M. L. "Pole-zero Decision Feedback Equalization with a Rapidly Converging Adaptive IIR Algorithm." **IEEE J. Selected Areas Commun.,** vol. 9, Aug. 1991. pp. 817–829.

(6) Kim Y., Moon J. "Noise-predictive Maximum-Likelihood Method Combined with Infinite Impulse Response Equalization." **IEEE Trans. on Magn.,** vol. 35, Nov 1999. pp. 4538–4543.

(7) Beliczynski B., Kale J., and Cain G. D. "Approximation of FIR by IIR Digital Filter An Algorithm Based on Balanced Model Reduction." **IEEE Trans. on Signal Processing,** vol.40, Mar. 1992. pp. 532–542.

(8) Moon J. H., Kang B. H., and Park P. "Direct Method for Converting FIR Filter with Low Nonzero Tap into IIR Filter." **IJCSE ,** vol. 2, no.1, Winter 2008.

(9) Hagenauer J., Hoeher P. "A Viterbi Algorithm with Soft-Decision Outputs and Its Applications." in **Proc. of Globecom'89,** Nov. 1989. pp. 1680–1686.

(10) Moon J., Zeng W. "Equalization for Maximum Likelihood Detector." **IEEE Trans. on Magn.,** vol. 31, no. 2, Mar. 1995. pp. 1083-1088.

(11) Choi J., Bouchard M., and Yeap T. H. "Decision Feedback Recurrent Neural Equalization with Fast Convergence Rate." **IEEE Trans. on Neural Networks**, vol. 16, no. 3, May 2005. pp. 699-708.

(12) Osawa H., Hino M., Shinohara N., Okamoto Y., Nakamura Y., and Muraoka H. "Simplified Neural Network Equalizer with Noise Whitening Function for GPRML System." **IEEE Trans. on Magn.,** Vol. 44, no. 11, Nov. 2008. pp. 3777-3780.

(13) Tyner D. J., Proakis J. G. "Partial Response Equalizer Performance in Digital magnetic Recording Channels." **IEEE Trans. on Magn.,** vol. 29, no. 6, Nov. 1993. pp. 4194–4208.

(14) Richardson T.J., Shokrollahi M.A., and Urbranke R.L. "Design of Capacity-Approaching Irregular Low-Density Parity-Check Codes." **IEEE Trans. Information Theory,** vol. 47, Feb. 2001. pp. 619-637.